Particle-specific toxicity of copper nanoparticles to soybean (Glycine max L.) effects of nanoparticle concentration and natural organic matter

Xiao, Y.L.; Tang, W.; Peijnenburg, W.J.G.M.

Environmental Toxicology

Particle-Specific Toxicity of Copper Nanoparticles to Soybean (*Glycine max* L.): Effects of Nanoparticle Concentration and Natural Organic Matter

Yinlong Xiao,[a,*,1] Wei Tang,[a,1] and Willie J. G. M. Peijnenburg[b,c]

[a]College of Environmental Sciences, Sichuan Agricultural University, Chengdu, PR China
[b]Institute of Environmental Sciences, Leiden University, Leiden, The Netherlands
[c]National Institute of Public Health and the Environment, Center for the Safety of Substances and Products, Bilthoven, The Netherlands

Abstract: For the soluble metallic nanoparticles (NPs), which forms (particles [$NP_{(particle)}$] vs. dissolved ions [$NP_{(ion)}$]) are the main cause of toxicity of the NP suspension ($NP_{(total)}$) remains uncertain. In the present study, soybean was exposed to Cu NPs in a hydroponic system to determine how natural organic matter (NOM; 10 mg/l) and concentration of Cu $NP_{(total)}$ (2–50 mg/l) affect the relative contributions of Cu $NP_{(particle)}$ and Cu $NP_{(ion)}$ to the overall toxicity. We found that NOM mitigated the phytotoxicity of Cu $NP_{(particle)}$ more significantly than that of Cu salt. When no NOM was added, Cu $NP_{(particle)}$ rather than Cu $NP_{(ion)}$ was the main contributor to the observed toxicity regardless of the concentration of Cu $NP_{(total)}$. However, NOM tended to reduce the relative contribution of Cu $NP_{(particle)}$ to the toxicity of Cu $NP_{(total)}$. Especially at a low concentration of Cu $NP_{(total)}$ (2 mg/l), the toxicity of Cu $NP_{(total)}$ mainly resulted from Cu $NP_{(ion)}$ in the presence of NOM (accounting for $\geq$70% of the overall toxicity). This might be attributable to the combined effects of increased dissolution of Cu NPs and steric-electrostatic hindrance between Cu $NP_{(particle)}$ and the soybean roots caused by NOM. Fulvic acids (FAs) tended to reduce the role of Cu $NP_{(particle)}$ in the overall toxicity more effectively than humic acids (HAs), which might partially be due to the higher extent of Cu NP dissolution on FA treatment than in HA treatment. Our results suggest that because of the relatively low metallic NP concentration and the presence of NOM in natural water, $NP_{(ion)}$ are likely problematic, which can inform management and mitigation actions. *Environ Toxicol Chem* 2021;40:2825–2835. © 2021 SETAC

Keywords: Copper nanoparticles; Natural organic matter; Behaviors; Time-weighted average concentration; Particle-specific toxicity

INTRODUCTION

The widespread production and application of metallic nanoparticles (NPs) have raised considerable concerns. Some metallic NPs, like Cu, Ni, and Zn, are expected to undergo dissolution after being released into aquatic environments (Hedberg et al., 2019; Z. Wang et al., 2016). This makes the toxicity mechanisms of metallic NPs complicated. Currently, there is no consistent conclusion in terms of the main cause of the toxicity of metallic NPs. Both NPs themselves (designated as $NP_{(particle)}$ hereafter) and dissolved ions shedding from NPs (designated as $NP_{(ion)}$ hereafter) have been reported to be

mainly responsible for the overall toxicity induced by NP suspensions (designated as $NP_{(total)}$ hereafter; Jeong et al., 2018; Ke et al., 2017; Qiu & Smolders, 2017; Rippner et al., 2018; Z. Zhang et al., 2018). In general, there are two commonly used methods for investigating the main cause underlying the toxicity of $NP_{(total)}$. One is to directly compare the toxicity of $NP_{(total)}$ with that of corresponding metal salts at equivalent metal molar concentrations (Asadishad et al., 2018; Bollyn et al., 2018; Z. Zhang et al., 2018), and the other is to distinguish between the toxic effects of $NP_{(total)}$ and of $NP_{(ion)}$ at merely a specific concentration of $NP_{(total)}$ (e.g., at the median effective concentration [EC50] and the median lethal concentration of $NP_{(total)}$; Wu et al., 2020; Xiao, Peijnenburg, et al., 2018; Zhai et al., 2017). In the former case, the relative contributions of $NP_{(particle)}$ and $NP_{(ion)}$ to the overall toxicity cannot be directly assessed because the corresponding dissolution profiles of metallic NPs are not quantified, while in the latter case the importance of the factor of NP concentration in

2826

Environmental Toxicology and Chemistry, 2021;40:2825–2835—Y. Xiao et al.

altering the physicochemical characteristics of NPs (e.g., dissolution rate and extent of aggregation), and consequently the roles of $NP_{(particle)}$ and $NP_{(ion)}$ in the observed toxicity, is ignored. Thereby, the physicochemical characteristics of metallic NPs at each individual NP concentration for exposure need to be comprehensively determined when assessing the relative contributions of $NP_{(particle)}$ and $NP_{(ion)}$ to the overall toxicity.

Natural organic matter (NOM) is ubiquitous in the environment and can affect the extrinsic physicochemical properties of metallic NPs. On the one hand, NOM has the potential to change surface properties of NPs through adsorption on the NPs, leading to inhibition or promotion of aggregation of the NPs (L. Wang et al., 2015; X. Wang et al., 2018; Xiao, Vijver, et al., 2018). On the other hand, NOM can affect the dissolution process of the soluble metallic NPs by blocking oxidation sites of the NPs after NOM adsorption and/or through ligand exchange (Azimzada et al., 2017; Collin et al., 2016; Yang et al., 2014). Consequently, the bioavailability of $NP_{(particle)}$ and $NP_{(ion)}$ to organisms may be significantly affected by NOM. Humic acids (HAs) and fulvic acids (FAs) are the major constitutes of NOM, accounting for approximately 50% of the total dissolved organic matter in surface waters (Chow et al., 2004; Hong & Elimelech, 1997; Ma et al., 2001). Moreover, HAs and FAs have large molecular masses, and they mainly contain aromatic carbons with phenolic structures, exhibiting a high ability to complex metals and to adsorb hydrophobic compounds (He et al., 2017; Pinchao et al., 2021). Therefore, HAs and FAs have been widely adopted as the model NOM to study. However, even for the same NPs, the effects of HAs and FAs on their behaviors and toxicity may be vastly different because HAs and FAs have different physicochemical properties (e.g., molecular weight, chemical composition, and functional groups; Erhayem & Sohn, 2014; Furman et al., 2013; E. X. Shang et al., 2017; W. Zhang et al., 2013). The different impacts of HAs and FAs on the behaviors (e.g., aggregation and dissolution processes) of NPs potentially result in varying bioavailability of $NP_{(particle)}$ and $NP_{(ion)}$ to organisms and ultimately alter their roles in overall toxicity induced by $NP_{(total)}$. However, to the best of our knowledge, none of the published studies involved in determining the main cause of toxicity of $NP_{(total)}$ have distinguished the specific effects of HAs and FAs on the relative importance of $NP_{(particle)}$ and $NP_{(ion)}$ in overall toxicity.

Copper-based NPs, as one of the five most widely used NPs, have been commonly applied in numerous products, such as pesticides, fungicides, catalyst, inks, plastics, and fuel cells (Leitch et al., 2012; Tegenaw et al., 2015). Meanwhile, Cu-based NPs have been confirmed to be highly toxic to plants and may transfer to higher trophic levels (Keller et al., 2017; Peng, Duan, et al., 2015; Peng et al., 2017; Wang, Xie, et al., 2012). The objective of the present study was to improve the understanding of the roles of Cu $NP_{(particle)}$ and Cu $NP_{(ion)}$ in the overall toxicity induced by Cu $NP_{(total)}$ through answering the following two questions: How do Cu NP concentrations affect the relative contributions of Cu $NP_{(particle)}$ and Cu $NP_{(ion)}$ to the overall toxicity? And to what extent can HAs and FAs alter the roles of Cu $NP_{(particle)}$ and Cu $NP_{(ion)}$ in the overall toxicity? In addition, the physicochemical characteristics of Cu NPs on different concentrations of Cu $NP_{(total)}$ and NOM treatments were integrated with the toxicity assessments to gain insight into the possible mechanisms underlying the effects of the concentrations of Cu $NP_{(total)}$ and NOM on the relative contributions of Cu $NP_{(particle)}$ and Cu $NP_{(ion)}$ to the overall toxicity. Soybean was selected to be the representative plant because it is the fifth most produced crop and accounts for 30% of the global production of vegetable oil (Rossi et al., 2018).

MATERIALS AND METHODS

Materials

Copper NPs (purity 99.9%, size range 10–30 nm, surface area ~30 m^2/g, shape spherical) and FAs were purchased from Macklin Biochemical. The Cu standard solution (GSB04-1725-2004) was obtained from the Analysis and Testing Center of the National Nonferrous Metals and Electronic Materials. In the present study, $CuSO_4 \cdot 5H_2O$, KH_2PO_4, $Ca(NO_3)_2 \cdot 4H_2O$, $MgSO_4 \cdot 7H_2O$, KNO_3, and the other chemicals used were of at least analytic grade purity and provided by Sinopharm Chemical Reagent; HAs were obtained from the Aladding Industrial Corporation. The HAs and FAs used in the present study have been widely characterized by other studies, and it is evident that the chemical characteristics of HAs are significantly different from those of FAs (e.g., the molecular weight of HAs is much higher than that of FAs, 2485 vs. 308 Da; Meng et al., 2017; Q. Zhang et al., 2017).

Toxicity tests

A stock Cu NP suspension (200 mg/l) was freshly prepared in deionized water after sonicating in a water bath for 20 min. The stock solutions of HAs and FAs were prepared by dissolving their powders in deionized water, adjusting the pH to 7.8 with 0.1 M sodium hydroxide solution, stirring overnight, and filtering through a 0.2-µm cellulose acetate membrane. The stock NOM solutions were stored at 4 °C before use. The concentrations of HAs and FAs were based on the total organic carbon (TOC) contents, as measured by means of a TOC analyzer (TOC-VCPH; Shimadzu).

Soybean seeds (*Glycine max* L. cv. Nandou 12) were provided by Sichuan Engineering Research Center for Crop Strip Intercropping System. The seeds were disinfected with 0.5% (w/v) sodium hypochlorite solution for 20 min and then rinsed thoroughly with distilled water three times. Subsequently, the sterilized seeds were germinated on moistened filter papers in Petri dishes, which were covered with tinfoil for blocking light and cultured in a growth chamber at 25 °C for 5 days. The germinated seedlings with similar growth status were transplanted into 50-ml glass beakers filled with 20% strength Hoagland solution (Hoagland & Arnon, 1950). Before transplanting the seedlings, appropriate amounts of the stock suspensions of Cu NPs and NOM were introduced into the Hoagland medium to achieve the desired exposure concentrations of Cu NPs (i.e., 2, 5, 10, 20, and 50 mg/l) and NOM (10 mg/l). The NOM concentration of 10 mg/l used in the present study is in the concentration range of NOM commonly found in natural freshwaters (1–60 mg/l; Robertson

et al., 1999). The actual exposure concentrations versus the nominal exposure concentrations of Cu NPs are presented in Supporting Information, Table S1. The pH of the Hoagland solution after addition of the NPs and NOM was adjusted to 6.8 by 0.1 M NaOH or HCl. The treatments with soybean seedlings transplanted into the Hoagland solutions without the addition of Cu NPs were regarded as the control experiments. Hence, there were three control experiment setups (i.e., without the addition of NOM and with the addition of either HAs or FAs). Two seedlings were planted in each beaker filled with 25 ml of the Hoagland solution. Each treatment consisted of three replicates, and hence, there were six seedlings in total for each treatment. All the seedlings were cultured in the growth chamber at 25 °C under a 6000 lux light intensity for 6 days (16: 8 hour light: dark photoperiod). The beakers were sealed with perforated parafilm to avoid a high extent of evaporation while maintaining air circulation. The culture media were refreshed every 2 days by transplanting the soybean plants into beakers containing the freshly prepared growth media with Cu NPs at the desired concentrations. Every time before submerging the soybean roots into the newly prepared media, the roots were thoroughly rinsed with deionized water three times to remove the Cu adsorbed on the root surface. After a 6-day incubation, the root length of each seedling was measured. In the present study, the relative root elongation rate (RRE, percentage) was employed as the toxicological endpoint because RRE is a rapid and sensitive early warning of phytotoxicity resulting from external stressors (Y. Liu et al., 2016; Qiu & Smolders, 2017). It was determined according to the following equation:

$$\text{RRE (\%)} = \frac{RL_S}{RL_C} \times 100 \qquad (1)$$

In Equation 1, RL_S (centimeters) represents the taproot length of soybean seedling exposed to Cu NPs on different NOM treatments and RL_C (centimeters) is the taproot length of soybean seedling planted in the corresponding control solution.

Characterization of Cu NPs

Characterization of Cu NPs in the growth medium without plants was conducted. The morphology and primary size of the Cu NPs in MilliQ water and in the Hoagland solution were analyzed via transmission electron microscopy (TEM; JEOL 1010; JEOL). Nnano Measure 1.2 software (Fudan University, China) was used to analyze the particle distribution of the Cu NPs. Because the culture medium for soybean growth was refreshed every 48 hours, the incubation duration for characterization of the Cu NPs was also 48 hours. Hydrodynamic diameters of the Cu NPs with an initial concentration range from 2 to 50 mg/l in the culture media on various NOM treatments were determined in triplicate immediately after preparation (~1 hour for the preparation of Cu NP suspensions, which was therefore referred to as 1 hour hereafter) and after 2, 12, and 48 hours by dynamic light scattering analysis (Zetasizer HS 3000; Malvern Instruments). Meanwhile, zeta-potentials of the Cu NP suspensions were measured with a Zetasizer Nano apparatus at each sampling time point.

The concentration of Cu NP(total) (including both Cu NP(particle) and Cu NP(ion)) remaining in the water column and dissolution kinetics of Cu NPs at each individual concentration on various NOM treatments were determined during the 48 hours of incubation. At each sampling time point (1, 12, 24, and 48 hours after preparation), three independent Cu NP suspensions with the same Cu NP concentration and NOM treatment were performed as triplicates to analyze the concentrations of Cu NP(total) remaining in the water column and of Cu NP(ion). Specifically, a 5-ml suspension was carefully sampled from the position approximately 2 cm below the surface of each Cu NP suspension, which was then digested by concentrated nitric acid (65%) at room temperature for at least 1 day. After the digestion, the concentration of Cu NP(total) remaining in the water column was measured by inductively coupled plasma optical emission spectrometry (ICP-OES; iCAP 6300 DUO; Thermo). Moreover, a 10-ml sample was drawn from the water column of each Cu NP suspension, which was subsequently centrifuged at 16 089 *g* for 30 min; and then the supernatant was filtered through a syringe filter with a 0.02-μm pore diameter (Anotop 25; Whatman). The filtrates were digested by concentrated nitric acid and analyzed by ICP-OES for the Cu concentration, which represented the portion of Cu NP(ion). For quality assurance/control, Cu standard solution (GSB04-1725-2004), reagent blanks, and triplicate samples were measured every 25 samples. Furthermore, the Cu standard solution was also used to check the recovery of Cu after the filtration step, and the Cu recovery was in the range of 96 to 101%, confirming that there was no loss of Cu NP(ion) after passing through the syringe filter. After determining the concentration of Cu NP(ion) in the filtrates, the concentration of Cu NP(particle) remaining in the water column could be derived by subtracting the concentration of Cu NP(ion) from the concentration of Cu NP(total) measured at each sampling point.

Data analysis and statistics

In general, the observed toxicity of NP(total) can be determined from both the NP(particle) and NP(ion). The response-addition and the concentration-addition models are commonly used to predict the combined toxicity of mixed chemicals. The concentration-addition model is valid for the mixture of chemicals with a similar mode of action, while the response-addition model is fit for modeling the joint effects of chemicals with dissimilar modes of action. Although the precise mechanisms underlying the toxicity of NP(ion) and NP(particle) remain unclear, an increasing number of studies have found that the mode of action of NP(particle) differs from that of NP(ion) (Poynton et al., 2011; Rainville et al., 2014; Wan et al., 2019). Accordingly, the additive effects of Cu NP(particle) and Cu NP(ion) were fitted using the response-addition model on the basis of the assumption that the modes of action of Cu NP(particle) and Cu NP(ion) were dissimilar (Gong et al., 2019; Wang, Chen, et al., 2012):

$$\text{RRE}_{(total)}(\%) = \frac{\text{RRE}_{(ion)} \times \text{RRE}_{(particle)}}{100} \qquad (2)$$

2828

Environmental Toxicology and Chemistry, 2021;40:2825–2835—Y. Xiao et al.

In Equation 2, RRE$_{(total)}$, RRE$_{(ion)}$, and RRE$_{(particle)}$ represent the RRE values of soybean plants after exposure to Cu NP$_{(total)}$, Cu NP$_{(ion)}$, and Cu NP$_{(particle)}$, respectively. In the present study, RRE$_{(total)}$ could be determined experimentally (Equation 1), and RRE$_{(ion)}$ was derived from the dose–response curves of CuSO$_4$ toward RRE values of soybean plants on various NOM treatments (Equation 1). This allows us to directly calculate the RRE$_{(particle)}$ at any individual concentration of Cu NPs applied. It is worth noting that the concentrations of NP$_{(particle)}$ and NP$_{(ion)}$ in the water column are not constant over time because they are subject to change along with exposure time. Even though in most cases the toxicological response of organisms to contaminants cannot be expected to be a linear function of time and concentration (Atherley, 1985; Watanabe et al., 2018), the time-weighted average (TWA) concentration has been widely recommended to be a practical expedient to integrate the time and concentration of exposure cycles (Xiao, Peijnenburg, et al., 2018; Zhai et al., 2017). Hence, the expression of the exposure concentrations of Cu NP$_{(total)}$, Cu NP$_{(particle)}$, and Cu NP$_{(ion)}$ was based on the TWA concentrations, which can be calculated according to the following equation (Belgers et al., 2011):

$$C_{TWA} = \frac{\sum_{n=1}^{N}\left(\Delta T_n \frac{C_{n-1}+C_n}{2}\right)}{\sum_{n=1}^{N}\Delta T_n} \qquad (3)$$

In Equation 3, C$_{TWA}$ is the TWA concentration for exposure duration of T$_n$, n is the number of time interval, N is the total number of time intervals, and C$_{n-1}$ and C$_n$ are the analyte concentrations observed at the start and end of a time interval, respectively.

The EC50 values with the corresponding 95% confidence intervals (CIs) for CuSO$_4$, Cu NP$_{(total)}$, and Cu NP$_{(particle)}$ were calculated using the log (inhibitor) versus normalized response-variable slope function in GraphPad Prism 5. Statistical analysis was conducted using SPSS 16.0 for Windows (SPSS). One-way analysis of variance (ANOVA) with Tukey's post hoc test was used to examine the statistical differences of the measured hydrodynamic diameters and zeta-potentials of the Cu NP suspensions on different NOM treatments; the concentrations of Cu NP$_{(ion)}$, Cu NP$_{(total)}$, and Cu NP$_{(particle)}$ remaining in the water column at each individual Cu NP concentration on different NOM treatments; and the EC50 values of CuSO$_4$, Cu NP$_{(total)}$, and Cu NP$_{(particle)}$ on different NOM treatments.

Normality and homogeneity of variance were checked by Levene's test before one-way ANOVA. Statistical significance was accepted at $\alpha = 0.05$. The results were expressed as mean values ± standard deviation.

RESULTS AND DISCUSSION

Behaviors of Cu NPs

The TEM image of Cu NPs prepared in MilliQ water shows that the Cu NPs were spherical and 10 to 30 nm in size (Supporting Information, Figure S1A). In addition, it was clear that the Cu NPs aggregated drastically in the growth medium (Supporting Information, Figure S1B). The aggregation profiles of Cu NPs at 2 and 50 mg/l within 48 hours of incubation in the exposure medium on varying NOM treatments are presented in Table 1. Consistent with the conclusions reported by the majority of other studies (Kteeba et al., 2017; H. Shang et al., 2019), we found that both HAs and FAs at 10 mg/l significantly inhibited the aggregation of Cu NPs at an initial concentration of 2 mg/l (Table 1). The hydrodynamic diameter of the Cu NPs at 2 mg/l was maintained at approximately 450 nm after 48 hours of co-exposure with NOM, which was significantly lower than the hydrodynamic diameter of the Cu NP suspension without the addition of NOM ($p < 0.05$; Table 1). The zeta-potential of the Cu NP suspension was significantly decreased with the addition of NOM ($p < 0.05$; Table 1). Steric and electrostatic repulsions exerted by NOM absorbing on NPs might account for the enhanced stability of the Cu NPs (Li et al., 2018; Romanello & Fidalgo de Cortalezzi, 2013; W. Zhang et al., 2013). Interestingly, the zeta-potential of the Cu NP suspension at 2 mg/l with HAs was significantly lower than that with FAs within 48 hours of incubation ($p < 0.05$; Table 1). Other studies have commonly reported HAs to have a higher molecular weight and aromaticity than FAs, leading to a higher propensity for HAs to adsorb on NPs via hydrophobic and π–π interactions (Erhayem & Sohn, 2014; H. Shang et al., 2019; W. Zhang et al., 2013). This might consequently result in the lower zeta-potentials of Cu NP suspensions in the presence of HAs than in the presence of FAs. When the concentration of Cu NPs reached 50 mg/l, the stabilizing effect of NOM on the Cu NPs seemed to be reduced compared to the stabilizing effect of NOM on the Cu NPs at 2 mg/l. Similar to the Cu NPs without the addition of NOM, the Cu NPs at 50 mg/l with the addition

TABLE 1: Hydrodynamic diameter and zeta-potential of Cu nanoparticles (NPs) on different natural organic matter treatments

Treatment	Hydrodynamic diameter (nm)[a]				Zeta-potential (mV)[a]			
	1 h	2 h	12 h	48 h	1 h	2 h	12 h	48 h
2 mg Cu NPs/L	461 ± 60	785 ± 194	1193 ± 369	1516 ± 221	−14 ± 2	−14 ± 1	−13 ± 1	−11 ± 1
2 mg Cu NPs/L + HA	355 ± 33	423 ± 50*	428 ± 54*	433 ± 30*	−26 ± 1*,**	−24 ± 0*,**	−22 ± 0*,**	−22 ± 1*,**
2 mg Cu NPs/L + FA	386 ± 23	437 ± 24*	488 ± 34*	468 ± 85*	−23 ± 1*	−22 ± 0*	−18 ± 1*	−17 ± 1*
50 mg Cu NPs/L	785 ± 79	2348 ± 406	1880 ± 304	2016 ± 376	−20 ± 2	−18 ± 1	−16 ± 1	−16 ± 1
50 mg Cu NPs/L+HA	682 ± 63	1373 ± 402*	1226 ± 252*	1119 ± 274*	−28 ± 2*,**	−27 ± 2*	−26 ± 1*,**	−25 ± 1*,**
50 mg Cu NPs/L+FA	742 ± 67	1454 ± 295*	1321 ± 234	1495 ± 221	−25 ± 1*	−24 ± 2*	−21 ± 1*	−20 ± 1*

[a]Hydrodynamic diameter and zeta-potential are presented as mean ± standard deviation ($n = 3$).
*Significant difference between treatments with and without the addition of natural organic matter at each time point ($p < 0.05$).
**significant difference between treatments of humic acids and fulvic acids (10 mg/L) at each time point ($p < 0.05$). HA = humic acid; FA = fulvic acid.

of NOM also formed aggregates with sizes in the micrometer scale (Table 1). Especially for the treatment with FAs, there was no statistically significant difference of the hydrodynamic diameter from that in the absence of NOM after 12 hours of incubation (Table 1). The reduced stabilizing effect of NOM on the Cu NPs at a high concentration (i.e., 50 mg Cu NPs/l) was likely caused by a high frequency of collision for NPs, which consequently resulted in the swift homoaggregation of Cu NPs. In fact, Markus et al. (2015) found by means of modeling that for metallic NPs at a high concentration (≥10 mg/l), homoaggregation between NPs was the most important transformation process. Our results confirm that the stabilizing effect of NOM on metallic NPs depends on the NP concentration and the type of NOM.

It is clear that the dissolution profile of Cu NPs could be affected by the concentration of the Cu NPs and the type of NOM (Figure 1). On increasing the concentration of Cu NPs from 2 to 50 mg/l in the treatments without the addition of NOM, the percentage of Cu NP$_{(ion)}$ relative to the Cu NP$_{(total)}$ concentration decreased from 23.6 to 4.6% (Figure 1). Furthermore, the concentration of Cu NP$_{(ion)}$ after 48 hours was significantly increased by NOM at any Cu NP$_{(total)}$ concentrations applied in the present study compared to the concentration of Cu NP$_{(ion)}$ on the treatment without the addition of NOM ($p < 0.05$; Figure 1). Specifically, the percentages of Cu NP$_{(ion)}$ relative to the Cu NP$_{(total)}$ concentrations at 2, 5, 10, 20, and 50 mg/l were increased by 30.4, 15.8, 10.4, 6.9, and 2.8%, respectively, after 48 hours of incubation in the presence of HAs at 10 mg/l compared to the percentages of Cu NP$_{(ion)}$ in suspensions to which no NOM was added (Figure 1). The promoting effects of NOM on the dissolution of metal-based NPs have been widely reported (Rippner et al., 2018; L. Wang et al., 2015). It has been reported that the dissolution of Cu NPs

in the water compartment is an oxidative process following the reaction in Equation 4 (Z. Wang et al., 2016):

$$Cu^0 + \frac{1}{4}O_2(aq) + H^+(aq) \leftrightarrow Cu^+(aq) + \frac{1}{2}H_2O \qquad (4)$$
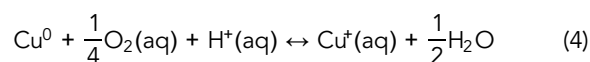
The mechanisms for NOM to enhance the dissolution of Cu NPs might include 1) the Cu NP$_{(ion)}$ has a strong potential to complex with functional groups of NOM through intra- and intermolecular chelation (L. Wang et al., 2015), which decreases the free Cu-ion concentration on the right-hand side of Equation 4 and further drives the particle dissolution (Zhao et al., 2017); 2) the deprotonation of carboxyl and phenolic groups of NOM increases the H$^+$ content in water (L. Wang et al., 2015; Zhao et al., 2017), which will consequently promote the dissolution rate of Cu NPs (Equation 4); and 3) NOM could inhibit the aggregation of Cu NPs and in turn enhance the dissolution of Cu NPs by maintaining the available surface area of Cu NPs for interaction with chemicals (e.g., organic matter, dissolved oxygen, and H$^+$; Arenas-Lago et al., 2019). Nonetheless, currently no consistent result in terms of the specific effect of NOM on the dissolution of metallic NPs can be drawn from the existing literature. In fact, promotion, inhibition, and even no effects of NOM on the dissolution of NPs have all been reported (Arenas-Lago et al., 2019; Rippner et al., 2018; E. X. Shang et al., 2017; L. Wang et al., 2015; Xiao, Vijver, et al., 2018; Zhao et al., 2017). These apparent conflicting results of different studies imply that more research in terms of the specific effects with the underlying mechanisms of NOM on the dissolution process of metallic NPs is needed. It is worth noting that the FAs induced a 2 to 12% higher dissolution of the Cu NPs than the HAs (Figure 1). Especially with the Cu NPs at 5 and 10 mg/l, the discrepancy
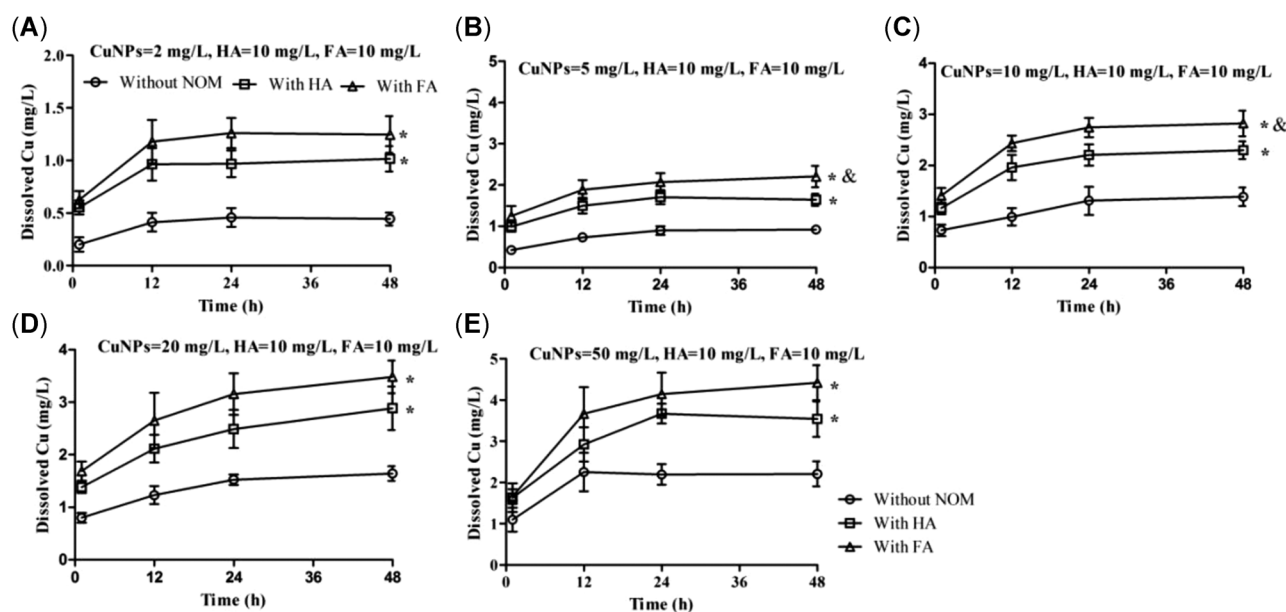

FIGURE 1: Concentration profiles of Cu ion nanoparticles (NP$_{(ion)}$) within 48 hours on different concentrations of Cu NPs and natural organic matter (NOM) treatments. (**A–E**) Dissolution profiles of Cu NPs with the initial concentrations of 2, 5, 10, 20, and 50 mg/l, respectively. Data are presented as mean ± standard deviation ($n = 3$). *Significant difference between treatments with and without the addition of NOM at 48 hours ($p < 0.05$), **significant difference between treatments of humic acids and fulvic acids ($p < 0.05$). HA = humic acid; FA = fulvic acid.

of dissolution between the treatments on the addition of FAs and HAs reached a statistically significant level ($p < 0.05$; Figure 1B and C). Similarly, Rippner et al. (2018) also found that the presence of FAs (60 mg C/l) induced an 11% higher extent of dissolution of CuO NPs (1.6 mg Cu/l) than the same concentration of HAs. H. Shang et al. (2019) concluded that NOM with a lower molecular weight would induce a higher extent of dissolution of CuO NPs because at an equivalent molar concentration NOM with a lower molecular weight had a higher number of functional groups (e.g., carboxylic and phenolic groups) devoted to ligand-assisted dissolution. The HAs and FAs used in the present study have been characterized by other studies, and it was found that the HAs had a much higher molecular weight than the FAs (2485 vs. 308 Da; Meng et al., 2017; Q. Zhang et al., 2017). Therefore, the lower extent of dissolution of Cu NPs on addition of the HAs likely resulted from the combined effects of lower binding affinity of the HAs with Cu NP$_{(ion)}$ and higher coating capability of the HAs for blocking oxidation sites on the Cu NPs compared to those of the FAs.

The concentrations of Cu NP$_{(total)}$ remaining in the aqueous phase on different Cu NP$_{(total)}$ concentrations and NOM treatments are shown in Figure 2. For the treatment without the addition of NOM, the percentage of Cu NP$_{(total)}$ remaining in the water phase relative to the concentration of Cu NP$_{(total)}$ after 48 hours gradually decreased from 48 to 9% on an increase of the concentration of Cu NP$_{(total)}$ from 2 to 50 mg/l (Figure 2). The copresence of NOM increased the concentration of Cu NP$_{(total)}$ remaining in the aqueous phase after 48 hours by 2- to 3-fold in comparison with the case where no NOM was added (Figure 2). The concentration of Cu NP$_{(particle)}$

maintaining in the aqueous phase was calculated by subtracting the concentration of Cu NP$_{(ion)}$ from the concentration of Cu NP$_{(total)}$ in the aqueous phase. The percentage of the concentration of Cu NP$_{(particle)}$ remaining in the suspension without NOM relative to the concentration of Cu NP$_{(total)}$ after 48 hours was gradually reduced from 24% when the concentration of Cu NP$_{(total)}$ was 2 mg/l to 5% when the concentration of Cu NP$_{(total)}$ equaled 50 mg/l (Figure 3). Moreover, NOM greatly increased the concentration of Cu NP$_{(particle)}$ in the aqueous phase after 48 hours (Figure 3). The concentration of Cu NP$_{(particle)}$ remaining in the aqueous phase with the NOM after 48 hours was approximately two to four times higher than in the exposure without the addition of NOM (Figure 3), with the exception of the co-exposure of Cu NP$_{(total)}$ at 2 mg/l and the FAs, where the concentration of Cu NP$_{(particle)}$ remaining in the aqueous phase was similar to that without the addition of NOM (Figure 3A).

Toxicity of Cu NPs on different NOM treatments

The dose–response curves of Cu NP$_{(total)}$ and CuSO$_4$ on different NOM treatments are presented in Figure 4. According to the dose–response relationships, the EC50 values of the Cu NP$_{(total)}$ and CuSO$_4$ were calculated (Table 2). The EC50 values for CuSO$_4$ were 6.36, 8.51, and 8.24 mg/l on the exposure scenarios without the addition of NOM and with the addition of 10 mg/l HAs and FAs, respectively. The dynamics of the exposure concentrations of Cu NP$_{(total)}$, Cu NP$_{(particle)}$, and Cu NP$_{(ion)}$ within 48 hours of exposure were analyzed using the TWA approach (Supporting Information, Table S2). The EC50 values for Cu NP$_{(total)}$ based on the TWA concentrations were
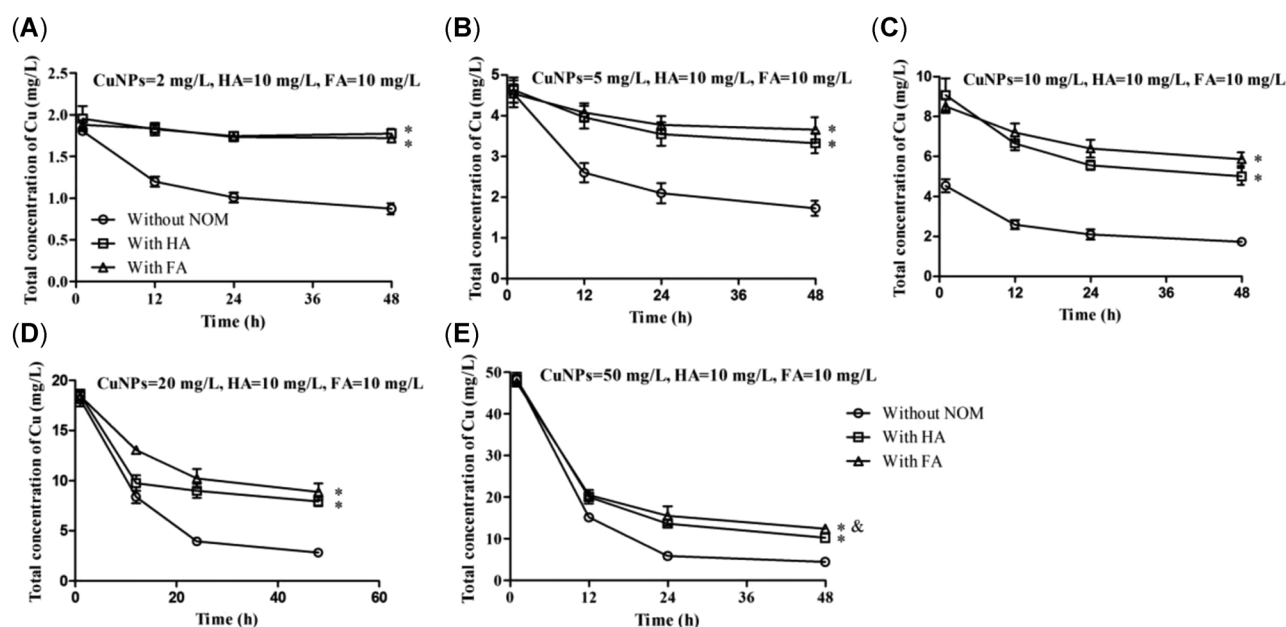

FIGURE 2: Concentrations of Cu total nanoparticles (NP$_{(total)}$) maintaining in the aqueous phase on different natural organic matter (NOM) treatments within 48 hours. (**A–E**) Concentrations of Cu NP$_{(total)}$ remaining in the water column with the initial concentrations of Cu NPs at 2, 5, 10, 20, and 50 mg/l, respectively. Data are expressed as mean ± standard deviation ($n = 3$). *Significant difference between treatments with and without the addition of NOM at 48 hours ($p < 0.05$), **significant difference between treatments of humic acids and fulvic acids ($p < 0.05$). HA = humic acid; FA = fulvic acid.
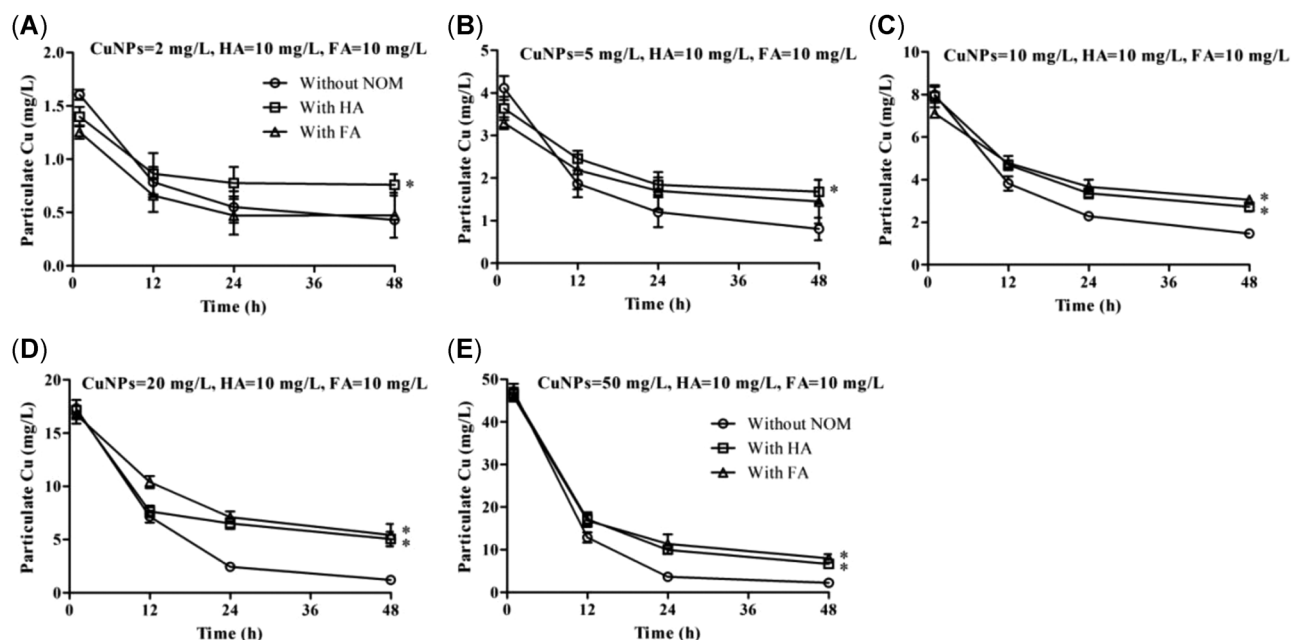
FIGURE 3: Concentrations of Cu particle (NP$_{(particle)}$) suspending in the aqueous phase on different natural organic matter (NOM) treatments within 48 hours. (**A–E**) Initial concentrations of Cu NPs at 2, 5, 10, 20, and 50 mg/l, respectively. Data are expressed as mean ± standard deviation ($n = 3$). *Significant difference between treatments with and without the addition of NOM at 48 hours ($p < 0.05$). HA = humic acid; FA = fulvic acid.

4.10, 11.04, and 11.69 mg/l on the treatments without the addition of NOM and with the addition of 10 mg/l HAs and FAs, respectively. The mitigating effects of HAs and FAs at 10 mg/l on the Cu-associated toxicity were similar (Table 2 and Figure 4). The specific effects of NOM on the toxicity induced by metallic NP$_{(total)}$ can result from the combined effects of NOM on the toxicity of NP$_{(particle)}$ and NP$_{(ion)}$. The dose–response curves expressed as the TWA concentrations for Cu NP$_{(particle)}$ derived from the response-addition model are shown in Figure 4C. Evidently, Cu NP$_{(particle)}$ exerted concentration-dependent toxicity (Figure 4C). It is interesting to note that NOM was much more effective at mitigating the toxicity of Cu NP$_{(particle)}$ than mitigating the toxicity of CuSO$_4$ (Table 2 and Figure 4A and C). Specifically, the addition of NOM markedly reduced the toxicity of Cu NP$_{(particle)}$, with the EC50 value decreasing from 5.46 mg/l (95% CI 3.49–8.55 mg/l) without the addition of NOM to 13.57 mg/l (95% CI 10.51–17.53 mg/l) and 26.38 mg/l (95% CI 12.50–55.65 mg/l) with the additions of HAs and FAs, respectively (Table 2 and Figure 4C). The marked reduction of the toxic effects of Cu NP$_{(particle)}$ on soybean root elongation when NOM was present might be attributed to the mechanism that NOM could reduce the bioavailability of NP$_{(particle)}$ to organisms through increasing electrostatic and steric repulsions between them (Peng, Zhang, et al., 2015; Z. Wang et al., 2016). To the best of our knowledge, very few studies have attempted to fit the dose–response curves for metallic NP$_{(particle)}$.

Relative contributions of Cu NP$_{(particle)}$ and Cu NP$_{(ion)}$ to toxicity

The combined effects of Cu NP concentrations and NOM on the relative contributions of Cu NP$_{(particle)}$ and Cu NP$_{(ion)}$ to the observed toxicity of Cu NP$_{(total)}$ are presented in Table 3. When no NOM was added to the exposure medium, Cu NP$_{(particle)}$ was the main contributor to the toxicity of Cu NP$_{(total)}$ to soybean seedlings, accounting for 63 to 74% of the overall toxicity (Table 3). Our results are consistent with the findings of several other studies, which reported that the phytotoxicity of Cu-based NPs mainly resulted from the presence of NP$_{(particle)}$ in the exposure medium in case no NOM was added (Ke et al., 2017; Margenot et al., 2018; Shi et al., 2014; Z. Zhang et al., 2018). Copper-based NPs can strongly adsorb on the root surface of plants (Nath et al., 2018; Peng et al., 2018; Z. Zhang et al., 2018). Some adsorbed NPs can enter into the intercellular space directly through cell wall pores and/or by inducing the formation of new and larger pores on cell walls (Vishwakarma et al., 2017; Yuan et al., 2016; P. Zhang et al., 2012). Schwabe et al. (2013) even found that CeO$_2$ NPs with a size >1 µm could accumulate in pumpkin root cells. Even though the accumulation profile of Cu NPs in the soybean seedlings was not determined in the present study, it is reasonable to deduce that the interactions between suspending Cu NPs and root cells may result in adsorption and even accumulation of Cu NPs in the soybean roots. The Cu NPs accumulating in plant roots may induce oxidative stress, resulting in damage and growth inhibition of the plants (Peng, Zhang, et al., 2015; Z. Zhang et al., 2018). The Cu-based NPs adhering to the plant root surface have the potential to block or clog the pores of cell walls, which could also inhibit plant growth by reducing the transport efficiency of water and nutrients from the exposure environment to the roots (Asli & Neumann, 2009; Dietz & Herth, 2011; Margenot et al., 2018; Servin & White, 2016). Consequently, Cu NP$_{(particle)}$ might induce toxic effects on soybean root elongation through the above-mentioned mechanisms.
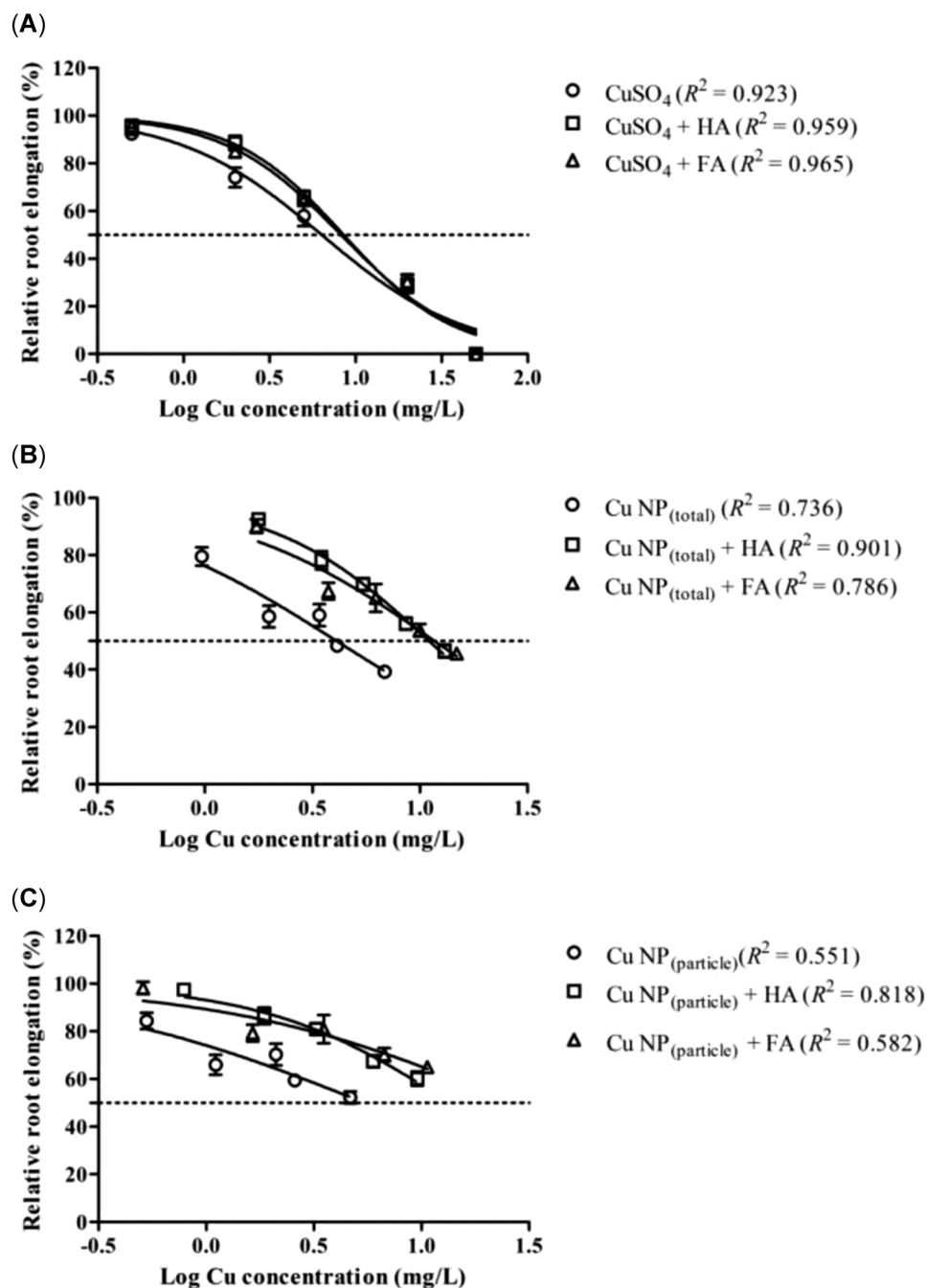
(A)

(B)

(C)

FIGURE 4: Dose–response curves of relative root elongation of soybean seedlings after 48 hours of exposure to different concentrations of $CuSO_4$ (A), Cu $NP_{(total)}$ (B), and Cu $NP_{(particle)}$ (C). The concentrations used for plotting the dose–response relationships of Cu $NP_{(total)}$ and Cu $NP_{(ion)}$ were expressed as time-weighted average concentrations. Data are expressed as mean ± standard deviation ($n = 6$). HA = humic acid; FA = fulvic acid.

On the other hand, when NOM was added into the exposure medium, the relative contribution of Cu $NP_{(particle)}$ to the observed toxicity exhibited a decreasing trend compared to the case in which no NOM was added. Especially when the concentration of Cu $NP_{(total)}$ was 2 mg/l, the relative contribution of Cu $NP_{(particle)}$ to the overall toxicity decreased from 69% without NOM to 30 and 23% on the addition of HAs and FAs, respectively. At 2 mg/l of Cu $NP_{(total)}$, approximately 20, 54, and 66% of the Cu NPs were dissolved on the treatments without and with the addition of HAs and FAs after 48 hours,

respectively (Figure 1A). Furthermore, NOM was much more effective at mitigating the toxicity of Cu $NP_{(particle)}$ than mitigating the toxicity of $CuSO_4$. Hence, the marked reduction of the relative contribution of Cu $NP_{(particle)}$ to the overall toxicity caused by NOM when Cu $NP_{(total)}$ was 2 mg/l might be attributed to the combined effects of the significantly increased concentration of Cu $NP_{(ion)}$ and the higher degree of mitigation of the toxic effects of Cu $NP_{(particle)}$ than Cu $NP_{(ion)}$ by NOM. When the concentration of Cu $NP_{(total)}$ was higher than 2 mg/l, the relative contribution of Cu $NP_{(particle)}$ to the overall toxicity

TABLE 2: Median effective concentration values of $CuSO_4$, Cu NP$_{(total)}$, and Cu NP$_{(particle)}$ expressed as time-weighted average concentrations

Treatment	EC50 (95% confidence intervals, mg/l)		
	$CuSO_4$	Cu NP$_{(total)}$	Cu NP$_{(particle)}$
No NOM	6.36 (5.16–7.84)	4.10 (3.46–4.86)	5.46 (3.49–8.55)
With HAs	8.51 (7.33–9.89)	11.04 (9.90–12.30)*	13.57 (10.51–17.53)
With FAs	8.24 (7.17–9.46)	11.69 (9.70–14.09)*	26.38 (12.50–55.65)

*Significant difference between treatments with and without the addition of natural organic matter at each time point ($p < 0.05$).
NP = nanoparticle; EC50 = median effective concentration; NOM = natural organic matter; HA = humic acid; FA = fulvic acid.

increased, which might be due to the fact that the extent of promoted dissolution of Cu NPs by NOM decreased at the higher concentrations of Cu NP$_{(total)}$ (Figure 1). It is interesting to note that the relative contribution of Cu NP$_{(ion)}$ to the overall toxicity on the addition of FAs tended to be higher than that with the addition of HAs (Table 3). This might partially be due to the promoting effect of FAs on the dissolution of Cu NPs being higher than the promoting effect of HAs (Figure 1). Moreover, the binding strength between the NOM with a lower molecular weight and metal ions has been reported to be weaker than the binding strength between the NOM with a higher molecular weight and metal ions (S. Liu et al., 2020). This may also assist in the explanation of the higher relative contribution of Cu NP$_{(ion)}$ complexed by FAs to toxicity than the relative contribution of Cu NP$_{(ion)}$ in case of the addition of HAs. Our results highlight the important role of NP$_{(ion)}$ in the overall toxicity when NOM was copresented, especially at a lower initial concentration of Cu NPs (≤ 2 mg/l).

Overall, the dose–response curves for Cu NP$_{(particle)}$ on different NOM treatments were fitted based on the TWA concentrations using the response-addition model. Evidently, NOM reduced the phytotoxicity of Cu NP$_{(particle)}$ much more markedly than that of Cu NP$_{(ion)}$. Moreover, the observed

TABLE 3: Relative contributions of Cu NP$_{(particle)}$ and Cu NP$_{(ion)}$ to the overall toxicity at different concentrations of Cu NP$_{(total)}$ and natural organic matter treatments analyzed by the response-addition model

Initial Cu NP$_{(total)}$ conc. (mg/l)		Relative toxic contribution (%)		
		No NOM	With HAs	With FAs
2	Particle	69 ± 12	30 ± 24	23 ± 23
	Ion	31 ± 12	70 ± 24	77 ± 23
5	Particle	74 ± 8	52 ± 26	56 ± 11
	Ion	26 ± 8	48 ± 26	44 ± 11
10	Particle	63 ± 9	57 ± 8	43 ± 24
	Ion	37 ± 9	43 ± 8	57 ± 24
20	Particle	69 ± 3	65 ± 4	55 ± 6
	Ion	31 ± 3	35 ± 4	45 ± 6
50	Particle	66 ± 3	63 ± 4	54 ± 3
	Ion	34 ± 3	37 ± 4	46 ± 3

Data are expressed as mean ± standard deviation ($n = 6$). Concentrations of both humic acids and fulvic acids in the present study were 10 mg/l.
NP = nanoparticle; NOM = natural organic matter; conc. = concentration; HA = humic acid; FA = fulvic acid; Particle = Cu NP$_{(particle)}$; Ion = Cu NP$_{(ion)}$.

toxicity of Cu NP$_{(total)}$ mainly resulted from Cu NP$_{(particle)}$ when no NOM was added. However, when NOM was present, the relative contribution of Cu NP$_{(particle)}$ to the overall toxicity was decreased. Especially at a low concentration of Cu NP$_{(total)}$ (2 mg/l), Cu NP$_{(ion)}$, rather than Cu NP$_{(particle)}$, was the major contributor to the overall toxicity. The alteration of the relative contributions of Cu NP$_{(particle)}$ and Cu NP$_{(ion)}$ to the observed toxicity of Cu NP$_{(total)}$ might result from the combined effects of the significantly increased dissolution of Cu NPs and steric-electrostatic hindrance between Cu NP$_{(particle)}$ and the soybean roots as caused by NOM. Compared to HAs, tended to induce a higher contribution of Cu NP$_{(ion)}$ to the observed toxicity, which might partially be due to the dissolution degree of Cu NPs on the FA treatment being higher than that on the HA treatment. Our results suggest that the metallic NP concentration and the type of NOM need to be considered when assessing the roles of NP$_{(particle)}$ and NP$_{(ion)}$ in the observed toxicity. The results of the present study also emphasize the importance of integrating the physicochemical characteristics of NPs into the interpretation of the toxicity pathways and mechanisms of metallic NPs.

REFERENCES

Arenas-Lago, D., Monikh, F. A., Vijver, M. G., & Peijnenburg, W. J. G. M. (2019). Interaction of zero valent copper nanoparticles with algal cells under simulated natural conditions: Particle dissolution kinetics, uptake and heteroaggregation. *Science of the Total Environment, 689,* 133–140.

Asadishad, B., Chahal, S., Akbari, A., Cianciarelli, V., Azodi, M., Ghoshal, S., & Tufenkji, N. (2018). Amendment of agricultural soil with metal nanoparticles: Effects on soil enzyme activity and microbial community composition. *Environmental Science & Technology, 52,* 1908–1918.

Asli, S., & Neumann, P. M. (2009). Colloidal suspensions of clay or titanium dioxide nanoparticles can inhibit leaf growth and transpiration via physical effects on root water transport. *Plant, Cell & Environment, 32,* 577–584.

Atherley, G. (1985). A critical review of time-weighted average as an index of exposure and dose and its key elements. *American Industrial Hygiene Association Journal, 46,* 481–487.

Azimzada, A., Tufenkji, N., & Wilkinson, K. J. (2017). Transformations of silver nanoparticles in wastewater effluents: Links to Ag bioavailability. *Environmental Science. NANO, 4,* 1339–1349.

Belgers, J. D. M., Aalderink, G. H., Arts, G. H. P., & Brock, T. C. M. (2011). Can time-weighted average concentrations be used to assess the risks of metsulfuron-methyl to *Myriophyllum spicatum* under different time-variable exposure regimes? *Chemosphere, 85,* 1017–1025.

Bollyn, J., Willaert, B., Kerré, B., Moens, C., Arijs, K., Mertens, J., Leverett, D., Oorts, K., & Smolders, E. (2018). Transformation–dissolution reactions partially explain adverse effects of metallic silver nanoparticles to soil nitrification in different soils. *Environmental Toxicology and Chemistry, 37,* 2123–2131.

2834

Environmental Toxicology and Chemistry, 2021;40:2825–2835—Y. Xiao et al.

Chow, C. W. K., Fabris, R., & Drikas, M. (2004). A rapid fractionation technique to characterise natural organic matter for the optimisation of water treatment processes. *Journal of Water Supply: Research and Technology—Aqua*, 53, 85–92.

Collin, B., Tsyusko, O. V., Starnes, D. L., & Unrine, J. M. (2016). Effect of natural organic matter on dissolution and toxicity of sulfidized silver nanoparticles to *Caenorhabditis elegans*. *Environmental Science. NANO*, 3, 728–736.

Dietz, K. J., & Herth, S. (2011). Plant nanotoxicology. *Trends in Plant Science*, 16, 582–589.

Erhayem, M., & Sohn, M. (2014). Stability studies for titanium dioxide nanoparticles upon adsorption of Suwannee River humic and fulvic acids and natural organic matter. *Science of the Total Environment*, 15, 468–469.

Furman, O., Usenko, S., & Lau, B. L. T. (2013). Relative importance of the humic and fulvic fractions of natural organic matter in the aggregation and deposition of silver nanoparticles. *Environmental Science & Technology*, 47, 1349–1356.

Gong, B., He, E., Qiu, H., Li, J., Ji, J., Zhao, L., & Cao, X. (2019). Phytotoxicity of individual and binary mixtures of rare earth elements (Y, La, and Ce) in relation to bioavailability. *Environmental Pollution*, 246, 114–121.

He, E., Qiu, H., Qiu, R., Rentenaar, C., Devresse, Q., & Van Gestel, C. A. N. (2017). Time-dependent uptake and toxicity of nickel to *Enchytraeus crypticus* in the presence of humic acid and fulvic acid. *Environmental Toxicology and Chemistry*, 36, 3019–3027.

Hedberg, J., Blomberg, E., & Wallinder, I. O. (2019). In the search for nanospecific effects of dissolution of metallic nanoparticles at freshwater-like conditions: A critical review. *Environmental Science & Technology*, 53, 4030–4044.

Hoagland, D. R., & Arnon, D. I. (1950). The water culture method for growing plants without soil. *California, Agricultural Experiment Station, Circular*, 347, 25–32.

Hong, S., & Elimelech, M. (1997). Chemical and physical aspects of natural organic matter (NOM) fouling of nanofiltration membranes. *Journal of Membrane Science*, 132, 159–181.

Jeong, J., Kim, S. H., Lee, S., Lee, D. K., Han, Y., Jeon, S., & Cho, W. S. (2018). Differential contribution of constituent metal ions to the cytotoxic effects of fast-dissolving metal-oxide nanoparticles. *Frontiers in Pharmacology*, 9 Article 15.

Ke, M., Zhu, Y., Zhang, M., Gumai, H., Zhang, Z., Xu, J., & Qian, H. (2017). Physiological and molecular response of *Arabidopsis thaliana* to CuO nanoparticle (nCuO) exposure. *Bulletin of Environmental Contamination and Toxicology*, 99, 713–718.

Keller, A. A., Adeleye, A. S., Conway, J. R., Garner, K. L., Zhao, L., Cherr, G. N., Hong, J., Gardea-Torresdey, J. L., Godwin, H. A., & Hanna, S. (2017). Comparative environmental fate and toxicity of copper nanomaterials. *NanoImpact*, 7, 28–40.

Kteeba, S. M., El-Adawi, H. I., El-Rayis, O. A., El-Ghobashy, A. E., Schuld, J. L., Svoboda, K. R., & Guo, L. D. (2017). Zinc oxide nanoparticle toxicity in embryonic zebrafish: Mitigation with different natural organic matter. *Environmental Pollution*, 230, 1125–1140.

Leitch, M. E., Casman, E., & Lowry, G. V. (2012). Nanotechnology patenting trends through an environmental lens: Analysis of materials and applications. *Journal of Nanoparticle Research*, 14, 1283–1305.

Li, S., Liu, H., Gao, R., Abdurahman, A., Dai, J., & Zeng, F. (2018). Aggregation kinetics of microplastics in aquatic environment: Complex roles of electrolytes, pH, and natural organic matter. *Environmental Pollution*, 237, 126–132.

Liu, S., Shirai, H., Zuo, J., Yang, X., Li, X., Kamruzzaman, M., & Fan, W. (2020). Characterizing the interactions between copper ions and dissolved organic matter using fluorescence excitation–emission matrices with two-dimensional Savitzky-Golay second-order differentiation. *Ecotoxicology and Environmental Safety*, 188 Article 109834.

Liu, Y., Baas, J., Peijnenburg, W. J. G. M., & Vijver, M. G. (2016). Evaluating the combined toxicity of Cu and ZnO nanoparticles: Utility of the concept of additivity and a nested experimental design. *Environmental Science & Technology*, 50, 5328–5337.

Ma, H., Allen, H. E., & Yin, Y. (2001). Characterization of isolated fractions of dissolved organic matter from natural waters and a wastewater effluent. *Water Research*, 35, 985–996.

Margenot, A. J., Rippner, D. A., Dumlao, M. R., Nezami, S., Green, P. G., Parikh, S. J., & McElrone, A. J. (2018). Copper oxide nanoparticle effects on root growth and hydraulic conductivity of two vegetable crops. *Plant and Soil*, 431, 333–345.

Markus, A. A., Parsons, J. R., Roex, E. W., de Voogt, P., & Laane, R. W. (2015). Modeling aggregation and sedimentation of nanoparticles in the aquatic environment. *Science of the Total Environment*, 506–507, 323–329.

Meng, F., Yuan, G., Wei, J., Bi, D., Ok, Y. S., & Wang, H. (2017). Humic substances as a washing agent for Cd-contaminated soils. *Chemosphere*, 181, 461–467.

Nath, J., Dror, I., Landa, P., Vanek, T., Kaplan-Ashiri, I., & Berkowitz, B. (2018). Synthesis and characterization of isotopically-labeled silver, copper and zinc oxide nanoparticles for tracing studies in plants. *Environmental Pollution*, 242, 1827–1837.

Peng, C., Chen, S., Shen, C., He, M., Zhang, Y., Ye, J., Liu, J., & Shi, J. (2018). Iron plaque: A barrier layer to the uptake and translocation of copper oxide nanoparticles by rice plants. *Environmental Science & Technology*, 52, 12244–12254.

Peng, C., Duan, D., Xu, C., Chen, Y., Sun, L., Zhang, H., Yuan, X., Zheng, L., Yang, Y., Yang, J., Zhen, X., & Shi, J. (2015). Translocation and biotransformation of CuO nanoparticles in rice (*Oryza sativa* L.) plants. *Environmental Pollution*, 197, 99–107.

Peng, C., Xu, C., Liu, Q., Sun, L., Luo, Y., & Shi, J. (2017). Fate and transformation of CuO nanoparticles in the soil–rice system during the life cycle of rice plants. *Environmental Science & Technology*, 51, 4907–4917.

Peng, C., Zhang, H., Fang, H., Xu, C., Huang, H., Wang, Y., Sun, L., Yuan, X., Chen, Y., & Shi, J. (2015). Natural organic matter–induced alleviation of the phytotoxicity to rice (*Oryza sativa* L.) caused by copper oxide nanoparticles. *Environmental Toxicology and Chemistry*, 34, 1996–2003.

Pinchao, G., Ortiz, L., Galeano, L., Hidalgo, A., & Ramíreza, J. (2021). Optimized CWPO oxidation of natural organic matter in continuous fixed bed reactor catalyzed by an extruded Al/Fe-PILC clay catalyst. *Journal of Environmental Chemical Engineering*, 9 Article 104634.

Poynton, H. C., Lazorchak, J. M., Impellitteri, C. A., Smith, M. E., Rogers, K., Patra, M., Hammer, K. A., Allen, H. J., & Vulpe, C. D. (2011). Differential gene expression in *Daphnia magna* suggests distinct modes of action and bioavailability for ZnO nanoparticles and Zn ions. *Environmental Science & Technology*, 45, 762–768.

Qiu, H., & Smolders, E. (2017). Nanospecific phytotoxicity of CuO nanoparticles in soils disappeared when bioavailability factors were considered. *Environmental Science & Technology*, 51, 11976–11985.

Rainville, L. C., Carolan, D., Varela, A. C., Doyle, H., & Sheehan, D. (2014). Proteomic evaluation of citrate-coated silver nanoparticles toxicity in *Daphnia magna*. *Analyst*, 139, 1678–1686.

Rippner, D. A., Green, P. G., Young, T. M., & Parikh, S. J. (2018). Dissolved organic matter reduces CuO nanoparticle toxicity to duckweed in simulated natural systems. *Environmental Pollution*, 234, 692–698.

Robertson, A. I., Bunn, S. E., Boon, P. I., & Walker, K. F. (1999). Sources, sinks and transformations of organic carbon in Australian floodplain rivers. *Marine & Freshwater Research*, 50, 813–829.

Romanello, M. B., & Fidalgo de Cortalezzi, M. M. (2013). An experimental study on the aggregation of TiO$_2$ nanoparticles under environmentally relevant conditions. *Water Research*, 47, 3887–3898.

Rossi, L., Sharifan, H., Zhang, W. L., Schwab, A. P., & Ma, X. M. (2018). Mutual effects and in planta accumulation of co-existing cerium oxide nanoparticles and cadmium in hydroponically grown soybean (*Glycine max* (L.) Merr.). *Environmental Science. NANO*, 5, 150–157.

Schwabe, F., Schulin, R., Limbach, L. K., Stark, W., Burge, D., & Nowack, B. (2013). Influence of two types of organic matter on interaction of CeO$_2$ nanoparticles with plants in hydroponic culture. *Chemosphere*, 91, 512–520.

Servin, A. D., & White, J. C. (2016). Nanotechnology in agriculture: Next steps for understanding engineered nanoparticle exposure and risk. *NanoImpact*, 1, 9–12.

Shang, E. X., Li, Y., Niu, J. F., Zhou, Y. J., Wang, T. Y., & Crittenden, J. C. (2017). Relative importance of humic and fulvic acid on ROS generation, dissolution, and toxicity of sulfide nanoparticles. *Water Research*, 124, 595–604.

Shang, H., Guo, H., Ma, C., Li, C., Chefetz, B., Polubesova, T., & Xing, B. (2019). Maize (*Zea mays* L.) root exudates modify the surface chemistry

of CuO nanoparticles: Altered aggregation, dissolution and toxicity. *Science of the Total Environment*, *690*, 502–510.

Shi, J., Peng, C., Yang, Y., Yang, J., Zhang, H., Yuan, X., Chen, Y., & Hu, T. (2014). Phytotoxicity and accumulation of copper oxide nanoparticles to the Cu-tolerant plant *Elsholtzia splendens*. *Nanotoxicology*, *8*, 179–188.

Tegenaw, A., Tolaymat, T., Al-Abed, S., El Badawy, A., Luxton, T., Sorial, G., & Genaidy, A. (2015). Characterization and potential environmental implications of select Cu-based fungicides and bactericides employed in U.S. markets. *Environmental Science & Technology*, *49*, 1294–1302.

Vishwakarma, K., Shweta, Upadhyay, N., Singh, J., Liu, S., Singh, V. P., Prasad, S. M., Chauhan, D. K., Tripathi, D. K., & Sharma, S. (2017). Differential phytotoxic impact of plant mediated silver nanoparticles (AgNPs) and silver nitrate (AgNO₃) on *Brassica* sp. *Frontiers in Plant Science*, *8* Article 1501.

Wan, J., Wang, R., Wang, R., Ju, Q., Wang, Y., & Xu, J. (2019). Comparative physiological and transcriptomic analyses reveal the toxic effects of ZnO nanoparticles on plant growth. *Environmental Science & Technology*, *53*, 4235–4244.

Wang, L., Habibul, N., He, D., Li, W., Zhang, X., Jiang, H., & Yu, H. (2015). Copper release from copper nanoparticles in the presence of natural organic matter. *Water Research*, *68*, 12–23.

Wang, X., Fan, W., Dong, Z., Liang, D., & Zhou, T. (2018). Interactions of natural organic matter on the surface of PVP-capped silver nanoparticle under different aqueous environment. *Water Research*, *138*, 224–233.

Wang, Z., Chen, J., Li, X., Shao, J., & Peijnenburg, W. J. G. M. (2012). Aquatic toxicity of nanosilver colloids to different trophic organisms: Contributions of particles and free silver ion. *Environmental Toxicology and Chemistry*, *31*, 2408–2413.

Wang, Z., Xie, X., Zhao, J., Liu, X., Feng, W., White, J. C., & Xing, B. (2012). Xylem- and phloem-based transport of CuO nanoparticles in maize (*Zea mays* L.). *Environmental Science & Technology*, *46*, 4434–4441.

Wang, Z., Zhang, L., Zhao, J., & Xing, B. (2016). Environmental processes and toxicity of metallic nanoparticles in aquatic systems as affected by natural organic matter. *Environmental Science. NANO*, *3*, 240–255.

Watanabe, H., Oda, S., Abe, R., Tanaka, Y., & Tatarazako, N. (2018). Comparison of the effects of constant and pulsed exposure with equivalent time-weighted average concentrations of the juvenile hormone analog pyriproxyfen on the reproduction of *Daphnia magna*. *Chemosphere*, *195*, 810–816.

Wu, J., Yu, Q., Bosker, T., Vijver, M. G., & Peijnenburg, W. J. G. M. (2020). Quantifying the relative contribution of particulate versus dissolved

silver to toxicity and uptake kinetics of silver nanowires in lettuce: Impact of size and coating. *Nanotoxicology*, *14*, 1399–1414.

Xiao, Y., Peijnenburg, W. J. G. M., Chen, G., & Vijver, M. G. (2018). Impact of water chemistry on the particle-specific toxicity of copper nanoparticles to *Daphnia magna*. *Science of the Total Environment*, *610–611*, 1329–1335.

Xiao, Y., Vijver, M. G., & Peijnenburg, W. J. G. M. (2018). Impact of water chemistry on the behavior and fate of copper nanoparticles. *Environmental Pollution*, *234*, 684–691.

Yang, X. Y., Jiang, C. J., Hsu-Kim, H., Badireddy, A. R., Dykstra, M., Wiesner, M., Hinton, D. E., & Meyer, J. N. (2014). Silver nanoparticle behavior, uptake, and toxicity in *Caenorhabditis elegans*: Effects of natural organic matter. *Environmental Science & Technology*, *48*, 3486–3495.

Yuan, J., He, A., Huang, S., Hua, J., & Sheng, G. D. (2016). Internalization and phytotoxic effects of CuO nanoparticles in *Arabidopsis thaliana* as revealed by fatty acid profiles. *Environmental Science & Technology*, *50*, 10437–10447.

Zhai, Y., Hunting, E. R., Wouterse, M., Peijnenburg, W. J. G. M., & Vijver, M. G. (2017). Importance of exposure dynamics of metal-based nano-ZnO, -Cu and -Pb governing the metabolic potential of soil bacterial communities. *Ecotoxicology and Environmental Safety*, *145*, 349–358.

Zhang, P., Ma, Y. H., Zhang, Z. Y., He, X., Zhang, J., Guo, Z., Tai, R. Z., Zhao, Y. L., & Chai, Z. (2012). Biotransformation of ceria nanoparticles in cucumber plants. *ACS Nano*, *6*, 9943–9950.

Zhang, Q., Qu, G., Wang, T., Li, C., Qiang, H., Sun, Q., Liang, D., & Hu, S. (2017). Humic acid removal from micro-polluted source water in the presence of inorganic salts in a gas-phase surface discharge plasma system. *Separation and Purification Technology*, *187*, 334–342.

Zhang, W., Rattanaudompol, U., Li, H., & Bouchard, D. (2013). Effects of humic and fulvic acids on aggregation of aqu/nC60 nanoparticles. *Water Research*, *47*, 1793–1802.

Zhang, Z., Ke, M., Qu, Q., Peijnenburg, W., Lu, T., Zhang, Q., Ye, Y., Xu, P., Du, B., Sun, L., & Qian, H. (2018). Impact of copper nanoparticles and ionic copper exposure on wheat (*Triticum aestivum* L.) root morphology and antioxidant response. *Environmental Pollution*, *239*, 689–697.

Zhao, J., Liu, Y., Pan, B., Gao, G., Liu, Y., Liu, S., Liang, N., Zhou, D., Vijver, M. G., & Peijnenburg, W. J. G. M. (2017). Tannic acid promotes ion release of copper oxide nanoparticles: Impacts from solution pH change and complexation reactions. *Water Research*, *127*, 59–67.